9th ANKARA INTERNATIONAL AEROSPACE CONFERENCE **AIAC-2017-048**
20-22 September 2017 - METU, Ankara TURKEY

EFFECT OF WING HEATING ON FLOW STRUCTURE OF LOW SWEPT DELTA WING

Gizem Şencan[1], Almıla Güvenç Yazıcıoğlu[2] and Mehmet Metin Yavuz[3]
Middle East Technical University
Ankara, Turkey

ABSTRACT

The effect of surface heating on flow structure over a 35° swept delta wing is characterized in a low speed wind tunnel using cross flow Particle Image Velocimetry (PIV) technique at the chordwise distance of x/C= 0.6. The experiments are conducted for the chord length based selected Reynolds numbers of Re=3000, Re=8000 and Re=10000 and the attack angles of α= 4°, 7°, 10° at three different heat flux conditions and with the absence of heating. The results indicate that the effect of wing heating on flow structure is limited to low Reynolds number cases, indicating different behaviors for vortex dominated and pre-stall regimes such that for the attack angles α= 4° and α= 7°, the wing heating causes drop in vorticity levels, shifting the concentrations toward the center of the planform, whereas at α=10° the movement of vorticity concentrations toward the leading edge of the planform with increase in levels is witnessed.

INTRODUCTION

Unmanned Air Vehicles (UAVs) and Micro Air Vehicles (MAVs), which can be represented by simplified planforms including nonslender delta wings, have many advantages in the defense industry and the field of aeronautics. The aerodynamics of these vehicles has been of considerable interest in recent years. These vehicles experiencing steady flight and/or defined maneuvers generate complex flow patterns, which must be well understood for the improvement in flight performances including enhancement in lift and reduction in buffeting.

Delta wings are non-traditional wing planforms that are separated into two groups including slender and nonslender wings according to the sweep angle. As stated in the study of Gursul, Wang and Vardaki (2007), the slender wings have a leading edge sweep more than 55°, while nonslender wings have leading-edge sweep less than or equal to 55°.

The flow over a delta wing at an angle of attack can be described as a pair of counter-rotating leading edge vortices (LEV's). The flow separates from the leading edge of the wing and forms a free shear layer that rolls up into a core, which generate counter-rotating vortices. Earnshaw and Lawford (1964) state that the maximum lift coefficients and stall angles of slender planforms are higher than the ones in nonslender wings. At sufficiently high attack angle, the core of vortex flow stagnates and undergoes a sudden expansion, called as vortex breakdown, which is commonly affected by the swirl level and the pressure gradient. (Gursul, 2005) The separated shear layer from the leading edge reattaches to the wing surface on nonslender delta wings, which is a phenomenon that may even occur after the vortex breakdown reaches the apex of the wing.(Gursul, Wang and Vardaki, 2007) The location of the vortex breakdown shifts towards the wing apex with increasing attack angle and the wing is said to be completely stalled where the three-dimensional surface separation appears on the planform. For

[1] Research Assistant, Mechanical Engineering Department., E-mail: gsencan@metu.edu.tr
[2] Assoc.Prof. Dr., Mechanical Engineering Department., E-mail: yalmila@metu.edu.tr
[3] Assoc.Prof. Dr., Mechanical Engineering Department., E-mail: ymetin@metu.edu.tr

nonslender delta wings, when the vortex breakdown reaches to the apex, primary attachment can still take place outboard of the centerline of the wing. This reattachment line moves inboard of the symmetry plane by increasing angle of attack. Laser illuminated flow visualization, Laser Doppler Anemometry and surface pressure measurements were performed over a 45° swept delta wing to investigate the flow structure. At sufficiently high angle of attack, three dimensional surface separation was obtained in the flow field.(Öztürk, Çelik, Tunç and Yavuz, 2012) Considering the flow over a 35° swept delta wing, three dimensional surface separation is witnessed at relatively lower attack angle α= 8°.(Yavuz and Rockwell, 2006) An experimental study over a 35° swept delta wing was performed where similar conclusions were drawn considering the surface separation and pre-stall regimes.(Zharfa, Ozturk, and Yavuz, 2016)

The flow over delta wings can be controlled either passively or actively. Especially for low swept delta wings, a few alternative flow control techniques have been performed to delay vortex breakdown and to prevent surface separation. In the passive control method, no energy input or feedback mechanism is required and it can be applied by changing the wing geometry. Active control techniques require energy input to manipulate the flow over the wing, including blowing and suction, small and large scale perturbations, and unsteady forcing. It was stated that the most effective passive control methods over delta wings are the application of additional control surfaces or increasing the wing flexibility.(Mitchell and Délery,2001) the effect of 60° swept canard on the vortex breakdown location was investigated in the study.(Myose et al., 1997) According to the results, the vortex breakdown delay was observed when the canard position reached to the original wing. In addition, the delay of stall was also obtained. Several studies were performed on moderate and high swept wings using a flexible material that prevented three dimensional surface separation. (Taylor, Wang, Vardaki, and Gursul, 2007) In addition, Vardaki et al. (2005) conducted to a study to understand the effect of buffeting over 50° and 60° swept delta wings. For nonslender delta wings, lift force enhancement and delay in stall were observed. They also found that, the excitation of shear layer instabilities and improving the shear layer reattachment causes increase in lift force. Several active control techniques were performed to prevent or delay three dimensional surface separation and vortex breakdown on nonslender delta wings. Pressure and PIV measurements were performed on a 50° swept delta wing by applying oscillatory blowing.(Williams, Wang, and Gursul, 2008) It was found that the stall was delayed and the suction from the upper surface was significantly improved by utilizing the wing oscillation. Zharfa et al. (2016) investigated the effect of steady blowing through the leading edge of a 35° swept delta wing to delay three-dimensional surface separation. In addition, the effect of unsteady leading edge blowing on the flow structure of a 45° swept delta wing was also investigated. (Cetin, Celik, and Yavuz, 2016)

Active flow control technique using thermal effects has not been commonly studied in the literature. Several studies have been conducted on square cylinders, triangular planforms, airfoils, and high sweep delta wings. According to the study, the effect of uniform surface temperature over NACA0012 airfoil on subsonic stall was investigated by both analytically and experimentally. By increasing temperature, the stall angle of the airfoil was reduced. In addition, the drag was increased while the lift coefficient was decreased with increasing heat. (Norton, Macha, and Young 1973) The effect of heating on leading edge vortices over a 60° high swept delta wing that heated over 600°K was investigated. As a result of the study, strong drag was obtained and increased with incidence. However, significant effect of heating on lift could not observed.(Marchman, 1975) An experimental study was performed on a 60-degree swept delta wing to prevent the vortex breakdown. The heat flux was applied from the suction side of the delta wing. As a result of the study, stationary vortex structure was obtained with increase in heat transfer coefficient.(Srigrarom and Lewpiriyawong 2004) According to the study, the aerodynamic efficiency improvement of a small-scale airfoil by heating the lower surface and cooling the upper surface of the airfoil was investigated. Delay of stall was observed only at low Reynolds number.(Kim, Rusak, and Koratkar 2003)

In the current study the effect of wing heating on flow structure over a 35° swept delta wing was characterized in a low speed wind tunnel using cross flow Particle Image Velocimetry

(PIV) technique at the chordwise distance of x/C= 0.6. The heating was provided in the form of uniform heat flux on the suction side of the wing, which corresponds to the upper surface as orientated in the wind tunnel. The experiments were conducted for the Reynolds numbers of Re=3000, Re=8000 and Re=10000 and the attack angles of α= 4°, 7°, 10° at three different heat flux conditions and also with the absence of heating.

METHODOLOGY

An open circuit, low-speed and suction type wind tunnel, located at the Fluid Mechanics Laboratory of the Mechanical Engineering Department at Middle East Technical University, was utilized to conduct the experiments. The dimensions of the test section are 750 mm width, 510 mm height, and 2000 mm length and the maximum turbulence intensity value in the test section was recorded as 0.9 %. The experiments were performed for the chord length based selected Reynolds numbers of Re=3000, Re=8000 and Re=10000 at the attack angles of α= 4°, 7°, 10°. A delta wing with a sweep angle of Λ=35° was used in the experiments. The chord length and the span of the wing were 105 mm and 300 mm, respectively. The wing was made of aluminum with a thickness of 5 mm and fabricated using a CNC machine. It was beveled at an angle of 45° from the leading edges on the windward side.

In the experiments, PIV technique was performed to quantify the velocity field. The schematic view of PIV setup is presented in Figure 2. A glycol based fog generator was used in the experiments. The flow was illuminated using double pulsed Nd:YAG laser that was positioned perpendicular to the freestream at the chordwise distance of x/C=0.6. Images of the tracer particles in the flow field region were captured by a CMOS camera, which was aligned perpendicular to the vertical side of the wind tunnel. A rectangular mirror with dimensions of 15x25 cm was located inside the test section with an orientation angle of 45° to the freestream in order to capture the flow field by the camera located outside the test section. The mirror was positioned at 9 chord distance downstream of the wing. A synchronizer was used to provide the connection between the camera and the laser. Insight 4G was the software that controlled the PIV setup. In the study, cross-correlation method was used to analyze the displacement of the seeding particles over time between the exposure of the first and second frame. The captured images were processed by Tecplot PIV Focus. Two hundred image pairs were taken for each of the investigated cases to obtain the time-averaged velocity field <V>. Streamlines <ψ> and the contours of constant non-dimensional axial vorticity (<ωC/U_∞>) were calculated after obtaining the time averaged velocity field.

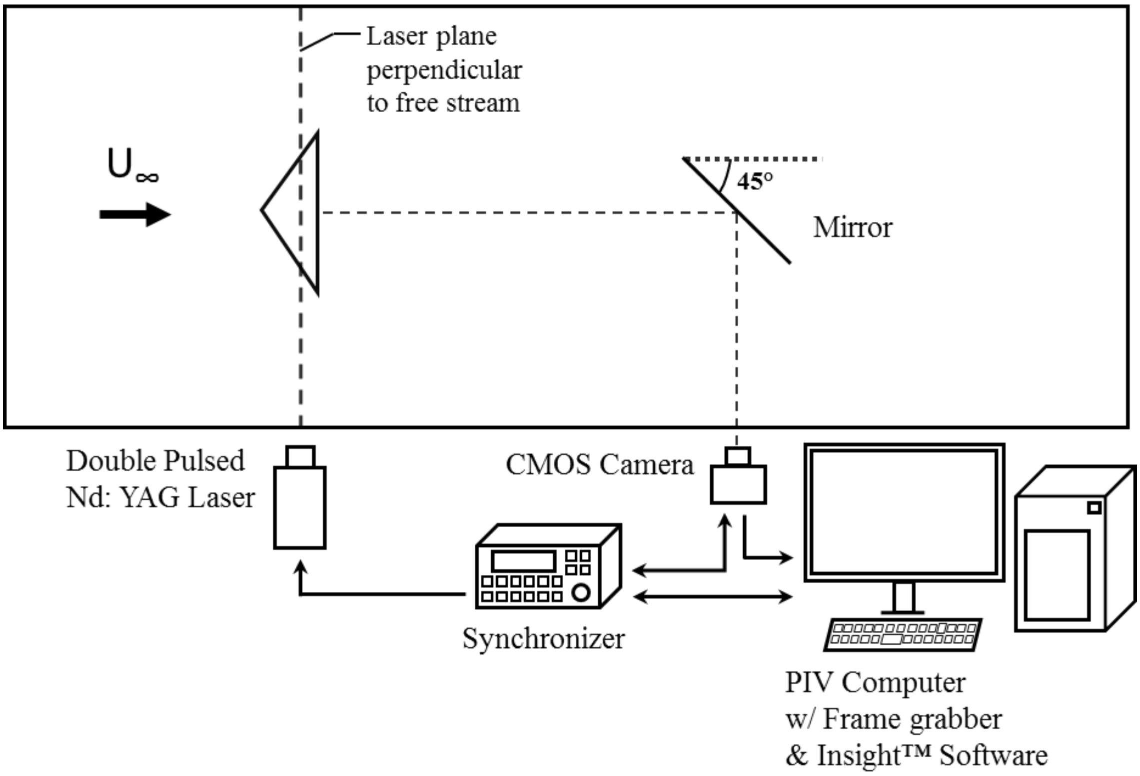

Figure 1: The schematic representation of cross flow PIV setup

A custom designed resistance wire heater was used to investigate the effect of heating on the flow structure. The heater was produced such that the resistance wire was coiled up with a 10 mm step around a mica sheet and positioned on the pressure side of the wing planform. By adjusting the operating voltage of the DC power supply, the heat rate supplied by the resistance heater onto the wing was controlled. Fifteen thermocouple wires were positioned into holes drilled with 2 mm depth to measure the surface temperature. Only half surface of the wing was used for positioning the thermocouples due to the fact that the flow structure over the wing was symmetric, which was confirmed with the preliminary experiments conducted. Agilent Data Logger was utilized to record the measured temperatures. The measurements were monitored at 1 Hz through the BenchLink Data Logger 3 software until steady-state conditions were achieved.

In this study, the heating conditions were quantified by taking the approximate temperature difference (ΔT) between the ambient temperature (T_∞) and the temperature of the heated wing surface (T_s) into account. Two sets of experiments were performed separately including steady-state and transient conditions. For the steady-state condition, three different heat flux condition were provided on the wing model; low, medium, and high, according to the corresponding power input values and the resulting temperature differences. The temperature differences were between $15 \leq \Delta T \leq 25$, $25 \leq \Delta T \leq 35$, and $35 \leq \Delta T \leq 45$ in the low, medium, and high heat flux sets, respectively. The velocity measurements were performed after all the readings from the thermocouples were stabilized and converged to a value over a period of time that corresponds to steady-state condition. For the transient condition, the velocity measurements were conducted until the steady-state condition was reached. For the high heat flux condition at $Re = 3000$ and $\alpha = 10°$, the PIV measurements were synchronized with eight different surface temperature values as shown in Figure 2.

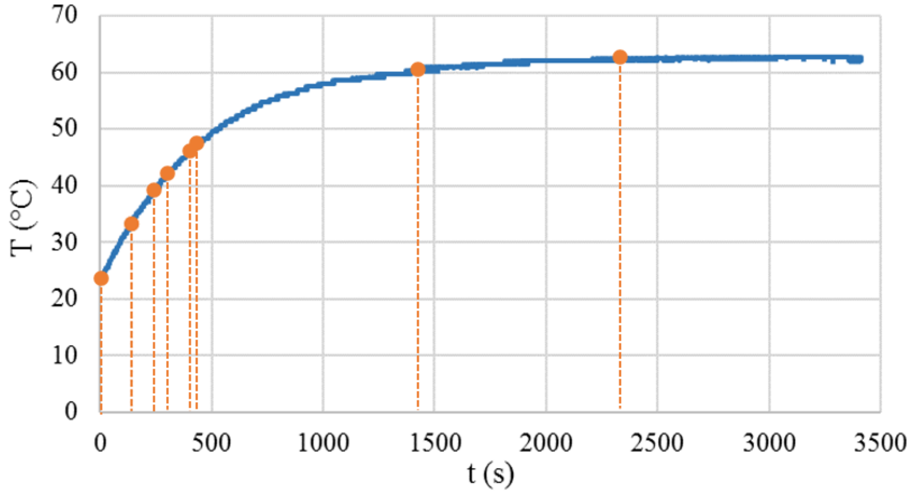

Figure 2: The temperature variation at transient condition for Re=3000 and α=10° with the corresponding PIV measurements synchronized with eight different surface temperatures.

RESULTS

The crossflow 2D PIV measurements were conducted to understand the effect of heating on the flow structure over a Λ=35° swept delta wing at the chordwise distance of x/C=0.6. First, the velocity measurements conducted for steady-state conditions are reported for the selected cases. Then, the measurements for the representative transient condition are presented in the proceeding section.

Particle Image Velocimetry measurement results for steady-state heating condition

Figure 3 and Figure 4 are constructed in the same format such that; the rows show the zero, low, medium and high heat flux conditions and columns represent the contours of constant non-dimensional vorticity, $<\omega C/U_\infty>$ for different cases. The contours of constant non-dimensional vorticity values are set with minimum and incremental values of 2 and 1 respectively ($[|<\omega C/U_\infty>|]_{min}=2$ and $\Delta[|<\omega C/U_\infty>|]=1$) for all cases in the Figures.

Comparison of constant non-dimensional vorticity contours, $<\omega C/U_\infty>$ for Re=3000 at the attack angles α=4°, 7°, 10° are demonstrated in Figure 3. A leading edge vortex pattern is observed in the flow field from zero to high heat flux condition for Re=3000 at α=4° as shown in the first column of Figure 3. For this case, the vorticity contours show that, the level of vorticity decreases by increasing heat flux. In addition, slight movement of vortex core toward the center plane is observed with increase in heat flux. When incidence angle reaches to α=7°, stronger vortex structure with relatively higher vorticity magnitudes is obtained compared to the α=4° case. The effect of heating on vorticity contours for α=7° is quite similar with the observations in α=4°, in which increase in heat flux causes a decrease in vorticity level and a shift in location of vortex core toward the center plane. However, the results are different for Re=3000 at α=10° compared to the results of attack angles α=4° and 7°. The vorticity concentration increases by increasing heat input at this high attack angle. In addition, elongated shear layer from the leading edge is obtained and as a result of this, the spatial extent of the vorticity contours increases with increase in heat flux. The vortex core slightly moves toward the leading edge of the planform.

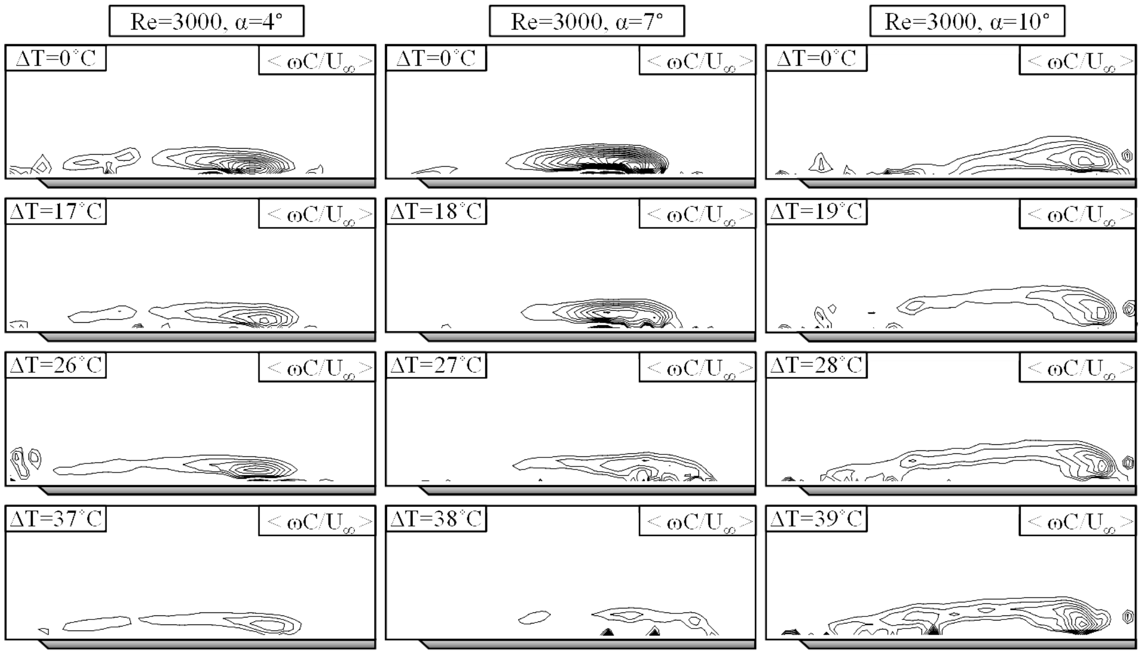

Figure 3: Comparison of non-dimensional vorticity contours for Re=3000 at the attack angles α= 4°, 7°, 10°: $[|\langle\omega C/U_\infty\rangle|]_{min}=2$, $\Delta[|\langle\omega C/U_\infty\rangle|]=1$

Comparison of non-dimensional vorticity contours at the attack angle α=10° for Re=3000, 8000, 10000 are presented in Figure 4. The rows indicate zero, low, medium and high heat flux conditions and the columns represent different Reynolds number cases. The vorticity contours show that, the effect of heating for α=10° at different Reynolds number values are similar. The level of the vorticity increases by increasing heat input for all cases. In addition, the vortex core slightly moves towards the leading edge of the wing.

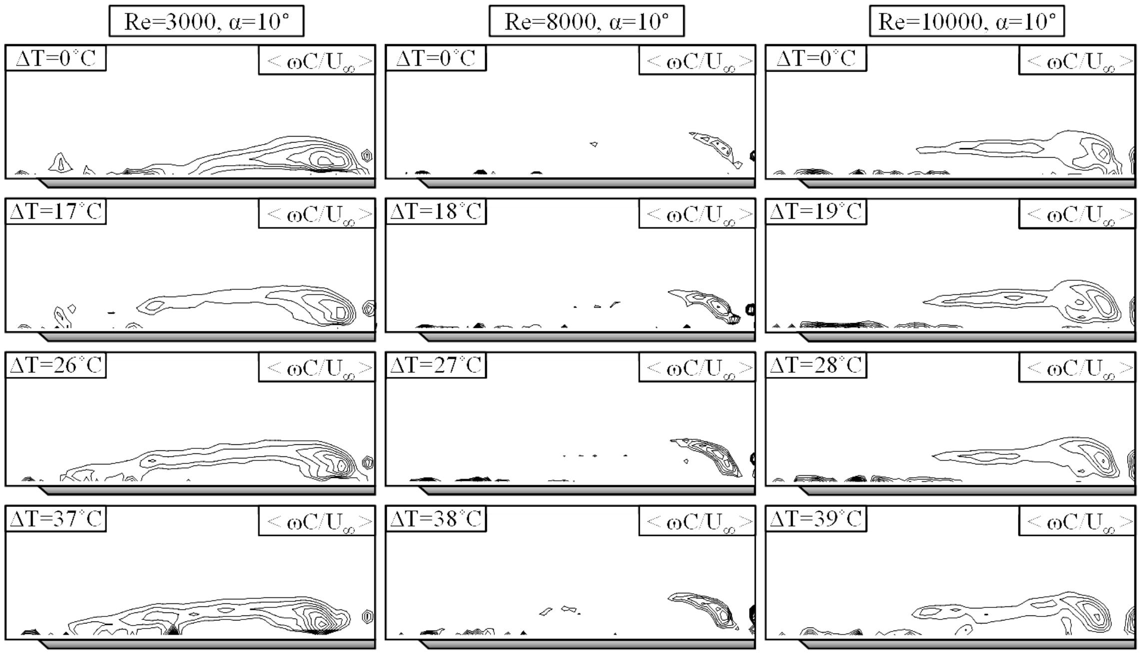

Figure 4: Comparison of non-dimensional vorticity contours for the attack angle α=10° at Re=3000, 8000, 10000: $[|\langle\omega C/U_\infty\rangle|]_{min}=2$, $\Delta[|\langle\omega C/U_\infty\rangle|]=1$

Particle Image Velocimetry measurement results for transient period

The time-averaged streamline patterns, <ψ> velocity vectors, <V> and non-dimensional vorticity contours, <ωC/U∞> for transient period are presented for no heat flux and all heat flux conditions. The constant non-dimensional vorticity contours are set with minimum and incremental values of 2 and 1 respectively ($[|\langle\omega C/U_\infty\rangle|]_{min}=2$ and $\Delta[|\langle\omega C/U_\infty\rangle|]=1$). Considering the results for Re=3000 and α=10˚ represented in Figure 5, the vorticity concentrations represent typical pre-stall condition, which are witnessed in all cases. The results of the measurements for transient period are obtained similar to steady-state condition for same Reynolds number and incidence. The vorticity contours show that, the level of the vorticity increases proximity of the wing surface as the heat flux increases. The spatial extent of the vorticity that corresponds to elongated shear layers from the leading edge increases when the heat input increases. Considering the patterns of streamline, velocity vectors, and vorticity contours, the location of the vortex core slightly shifts toward the leading edge by increasing heat flux.

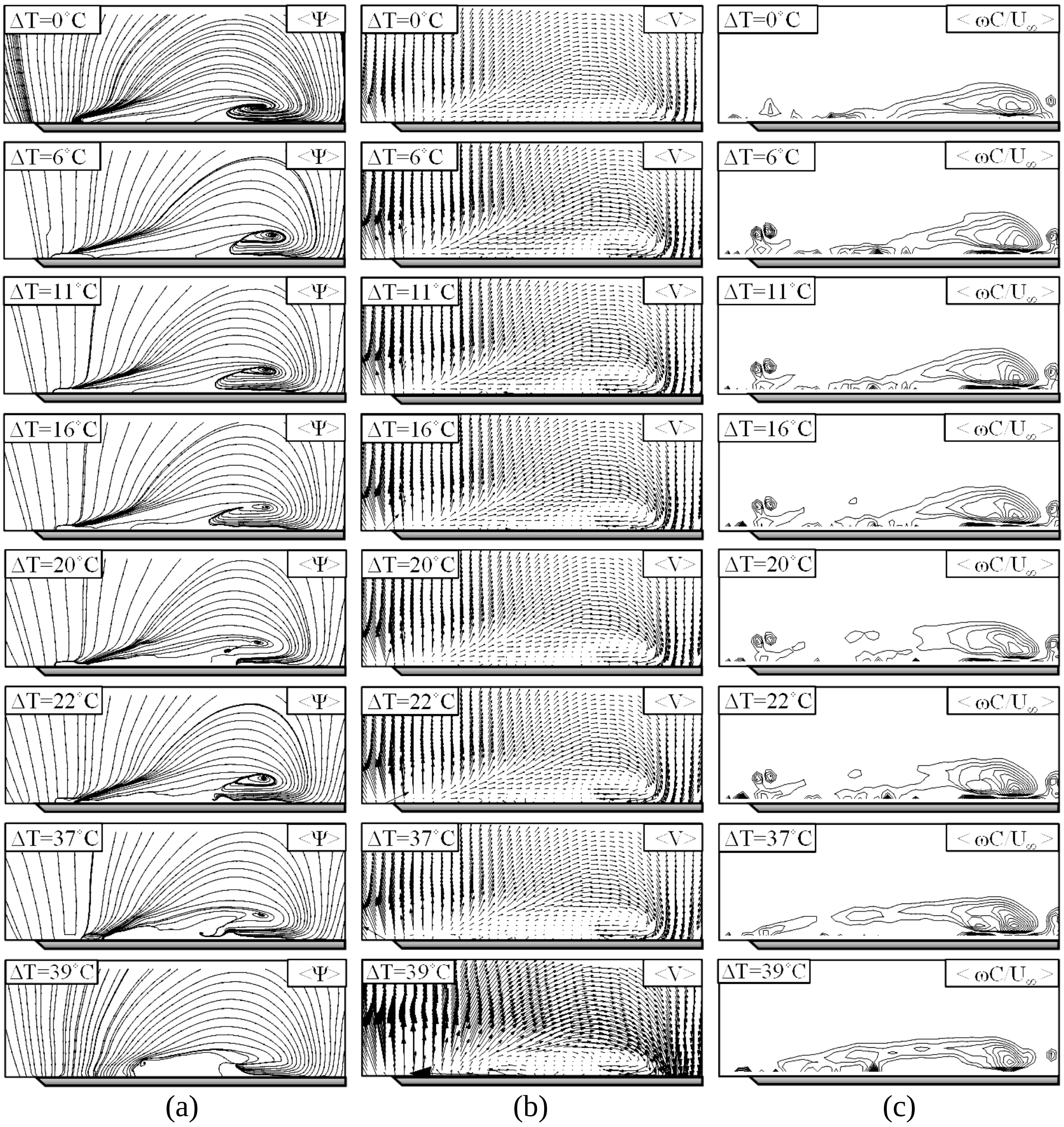

Figure 5: Comparison of (a) time-averaged streamline patterns, (b) velocity vector and (c) non-dimensional vorticity contours for transient measurement at Re=3000 and α=10°: $[|\langle\omega C/U_\infty\rangle|]_{min}=2$, $\Delta[|\langle\omega C/U_\infty\rangle|]=1$

Temperature measurements for steady-state heating condition

Data reduction:

The results of temperature measurements taken from fifteen thermocouples positioned in the delta wing are presented and discussed in detail. The calculations and discussions about plotted results are presented for the experimental matrix used in the steady state heating condition. The formulations of the calculations are given below.

The results of temperature measurements are used to calculate Grashof number, Gr in order to obtain the effect of heat transferred by natural convection. In addition, convection heat transfer coefficient h [W/m^2 K] and Nusselt number, Nu are also calculated using the temperature measurements.

Grashof number is a non-dimensional parameter that can be inferred as the ratio of buoyant forces to viscous forces and it is calculated as defined below.

$$\mathbf{Gr} = \frac{\mathbf{g \cdot \beta \cdot \Delta T \cdot C^3}}{\boldsymbol{\upsilon}^2} \tag{1}$$

Here, C [m] is the chord length, used as the characteristic length of the wing. The gravitational constant is represented as g, while β is defined as the inverse of the film (mean) temperature. ΔT [K] represents the temperature difference between the heated wing surface T_s and the ambient temperature T_∞ and $\boldsymbol{\upsilon}$ is defined as the kinematic viscosity of the convecting fluid.

In convection analyses, the relative magnitudes of Gr and Re are an indication of the relative importance of natural and forced convection. Natural convection effects are usually insignificant, when Gr/Re^2 << 1. This comparison is important when developing correlations based on experimental data. Although developing correlations is not the aim of the current work, according to the calculations for all cases, the maximum Gr/Re^2 value is 0.5 for the highest attack angle α=10° and lowest Reynold number Re=3000.

The amount of heat transferred per unit surface area, also known as heat flux, q" [W/m^2], is calculated using the electrical power input per unit heat transfer area of the wing surface. Electrical power is the product of voltage, *V*, in volts and electric current, I, in amperes using data taken from the DC power supply.

$$\mathbf{q}'' = \frac{\mathbf{V \cdot I}}{\mathbf{A}} \tag{2}$$

Convective heat transfer coefficient can be calculated with the knowledge of heat flux and the difference in temperature ΔT [K] between the heated wing surface T_s and the ambient temperature T_∞ as provided below.

$$\mathbf{h} = \frac{\mathbf{q}''}{\mathbf{\Delta T}} \tag{3}$$

Nusselt number is a non-dimensional parameter that can be inferred as the ratio of total convective heat transfer to conductive heat transfer across the solid-fluid boundary.

$$\mathbf{Nu} = \frac{\mathbf{h \cdot C}}{\mathbf{k}} \tag{4}$$

Here, C [m] is the chord length, used as the characteristic length of the wing. The thermal conductivity of the fluid k [W/mK] is obtained separately for each case according to the film temperature T_f defined below.

$$\mathbf{T_f} = \frac{\mathbf{T_s + T_\infty}}{\mathbf{2}} \tag{5}$$

Plot of temperature calculations:

In this section, in Figure 6, the relation between Nusselt number and Reynolds number at different angle of attack and heat flux conditions is presented.

The plot reveals that Nusselt number increases by increasing Reynolds number for all heat flux cases. In addition, when the heat rate increases from no heat flux to high heat flux case for each Reynolds number, Nusselt number also increases slightly in all cases, an expected result of the direct proportionality between Nusselt number and heat flux.

For all Reynolds number values, Nusselt number decreases when the attack angle increases. Nusselt number reaches its highest value in lowest angle of attack. Thus, for each Reynolds number, the highest Nusselt number values are obtained at α=4°. In addition, by increasing Reynolds number, Nusselt number increases for each angle of attack. Thus, the highest Nusselt number values are obtained at the highest Reynolds number and the lowest angle of attack.

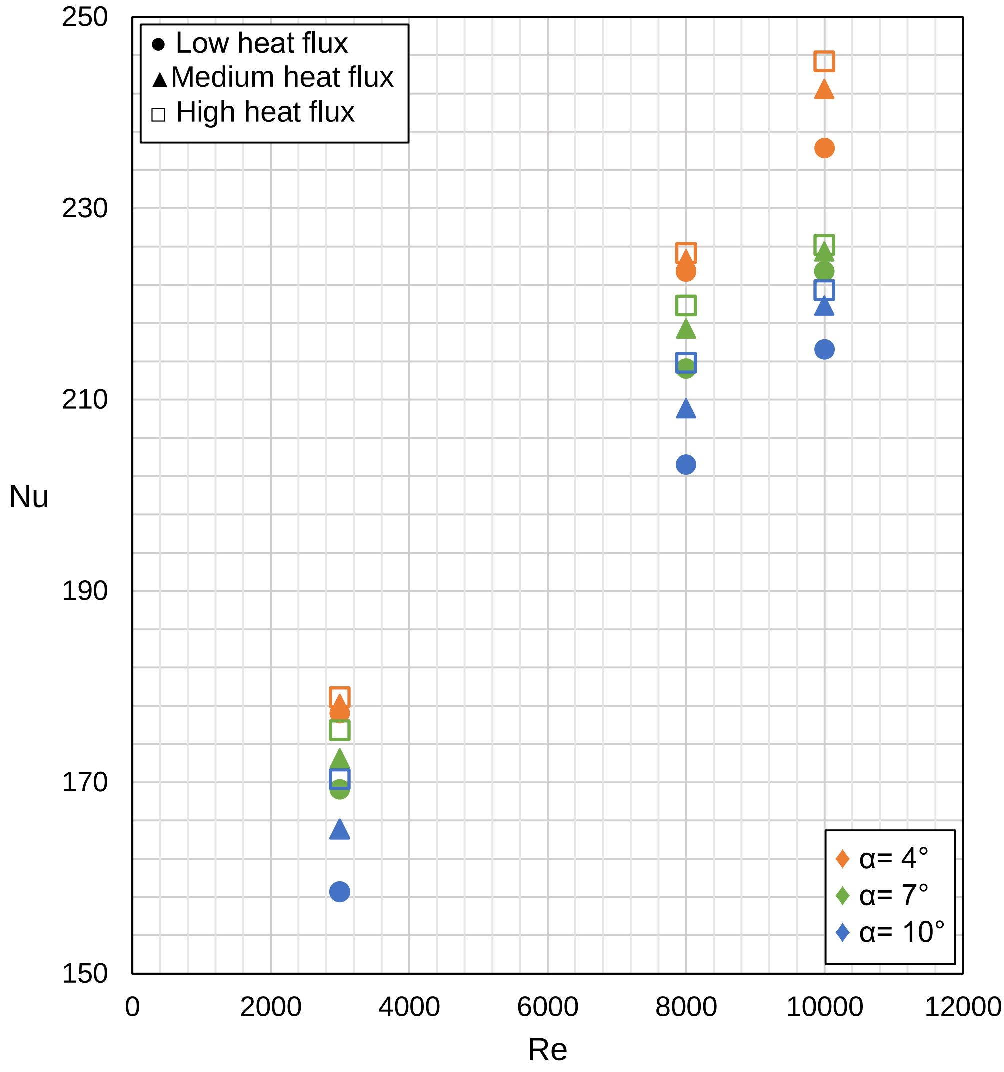

Figure 6: Nusselt number vs Reynolds number for low, medium, high heat flux cases at α= 4°, 7° and 10°

CONCLUSION

In this study, the effect of wing heating on flow structure of a 35° swept delta wing was investigated experimentally. According to the velocity measurement results, similar changes are obtained by increasing heat flux for attack angles α=4˚ and 7˚ in which the leading edge vortex structure dominates the flow over the wing. The location of the vortex core slightly moves towards the inboard of the symmetry plane with increase in heat flux. In addition, the level of the vorticity contours decreases by increasing heat input. The effects of heat input on flow structure at angle of attack α =10° are different compared to the results of attack angles α=4˚ and 7˚. This relatively high attack angle, α =10°, is considered as pre-stall condition where natural convection appears to be dominant as a result of the considerably low velocities existing on the wing. Thus, the flow structure could be energized by heating the surface of the wing for which the buoyant forces are considered to be responsible. As a result of that, the vortex core slightly moves towards the leading edge when the heat input increases. In addition, the vorticity levels increase in the vicinity of the vortex core and the shear layer elongates from the leading edge of the wing. For the transient period at Re=3000 and α=10˚, the vorticity contours show that, the level of the vorticity increases in the vicinity of the vortex core by increasing heat. The spatial extent of the vortex structure increases with observation of elongated shear layers from the leading edge of the wing. In addition, the reattachment location slightly shifts towards the leading edge.

According to the results of temperature measurements, Nusselt number increases at each angle of attack by increasing Reynolds number and increasing heat rate at all angles of attack. In addition, Nusselt number reaches its highest value in the lowest angle of attack that corresponds to α=4˚.

References

Earnshaw, P. B. and J. a Lawford. (1964) *"Low-Speed Wind-Tunnel Experiments on a Series of Sharp-Edged Delta Wings."* Aeronautical (3424).

Cetin, C., Celik, A., Yavuz, M. M. (2016) "*Düşük Ok Açılı Delta Kanat Akışının Zamana Bağlı Üfleme Tekniği ile Kontrolü*", VI. Ulusal Havacılık ve Uzay Konferansı, UHUK, September 28-30, Kocaeli, Turkey, Paper No: 2016-071.

Earnshaw, P. B. and J. a Lawford. (1964) *"Low-Speed Wind-Tunnel Experiments on a Series of Sharp-Edged Delta Wings."* Aeronautical (3424)

Gursul, I., R. Gordnier, and M. Visbal. (2005) *"Unsteady Aerodynamics of Nonslender Delta Wings."* Progress in Aerospace Sciences 41(7):515–57.

Gursul, I., Wang, Z. and Vardaki, E. (2007) "*Review of Flow Control Mechanisms of Leading-Edge Vortices.*" Progress in Aerospace Sciences 43(7–8):246–70.

Gursul, I. (2005) "*Review of Unsteady Vortex Flows over Slender Delta Wings.*" Journal of Aircraft 42(2):299–319.

Kim, J., Rusak, Z. and N. Koratkar. (2003) *"Small-Scale Airfoil Aerodynamic Efficiency Improvement by Surface Temperature and Heat Transfer."* AIAA Journal.

Marchman, JF. (1975) *"Effect of Heating on Leading Edge Vortices in Subsonic Flow."* Journal of Aircraft 12(2).

Mitchell, AM and J. Délery. (2001) *"Research into Vortex Breakdown Control."* Progress in Aerospace Sciences.

Myose, RY, S. Hayashibara, PC Yeong, and LS Miller. (1997) *"Effect of Canards on Delta Wing Vortex Breakdown During Dynamic Pitching."* Journal of Aircraft.

Norton, David J., John M. Macha, and James C. Young. (1973) *"Surface Temperature Effect on Subsonic Stall."* Journal of Spacecraft and Rockets 10(9):581–87.

Ol, Michael V. and Morteza Gharib. (2003) *"Leading-Edge Vortex Structure of Nonslender Delta Wings at Low Reynolds Number."* AIAA Journal 41(1):16–26.

Srigrarom, S. and N. Lewpiriyawong. (2004) *"Effect of Stationary Vortex to Heat Transfer on Delta Wings."* International Congress on Aeronautical Science.

Taylor, G., T. Schnorbus, and I. Gursul. (2003) *"An Investigation of Vortex Flows Over Low Sweep Delta Wings."* AIAA Aerospace Meeting and Exhibit (June).

Taylor, Gordon, Zhijin Wang, Eleni Vardaki, and Ismet Gursul. (2007) *"Lift Enhancement over Flexible Nonslender Delta Wings." AIAA Journal* 45(12):2979–93.

Vardaki, E., I. Gursul, G. S. Taylor, and Postgraduate Student. (2005) *"Physical Mechanisms of Lift Enhancement for Flexible Delta Wings." AIAA Paper* (January):1–13.

Vardaki, E., Z. Wang, and I. Gursul. (2008) "*Flow Reattachment and Vortex Re-Formation on Oscillating Low-Aspect-Ratio Wings." AIAA Journal* 46(6):1453–62.

Williams, NM, Z. Wang, and I. Gursul. (2008) "*Active Flow Control on a Nonslender Delta Wing.*" *Journal of Aircraft*.

Yaniktepe, B. and D. Rockwell. (2004) "*Flow Structure on a Delta Wing of Low Sweep Angle.*" *AIAA Journal* 42(3):513–23.

Yavuz, MM and D. Rockwell. (2006) "*Control of Flow Structure on Delta Wing with Steady Trailing-Edge Blow.*" *AIAA Journal* 44(3):493–501.

Zharfa, M., Ozturk, I., and Yavuz, M. M. (2016) "*Flow Structure on Nonslender Delta Wing: Reynolds Number Dependence and Flow Control*", AIAA Journal, Vol. 54, No. 3 pp. 880-897.